Efficient sub-wavelength light confinement using surface plasmon polaritons in tapered fibers

Fabrizio Renna[1], David Cox[2] and Gilberto Brambilla [1,*]

[1]*Optoelectronics Research Centre, University of Southampton, Southampton, SO17 1BJ, UK*
[2]*Advanced Technology Institute, University of Surrey, Guildford, GU2 7XH, UK*
[*]*Corresponding author:gb2@orc.soton.ac.uk*

Abstract: Light confinement to sub-wavelength spot sizes is proposed and realized in tapered optical fibers. To achieve high transmission efficiencies, light propagating along the taper is combined with the excitation of surface plasmon polaritons (SPP) at its tip.

OCIS codes: (230.1150) All-optical devices; (060.2340) Fiber optics components; (220.4000) Microstructure fabrication; (220.4241) Nanostructure fabrication.

References and links

1. D. Courjon and C. Bainier, "Near field microscopy and near field optics," Rep. Prog. Phys. **57,** 989-1028 (1994).
2. V. R. Almeida, Q. Xu, C.A. Barrios, and M. Lipson, "Guiding and confining light in void nanostructure," Opt. Lett. **29,** 1209-1211 (2004).
3. V. Veselago, "Electrodynamics of substances with simultaneously negative electrical and magnetical permeabilities," Sov. Phys. Usp. **10,** 509-514 (1968).
4. J. B. Pendry, "Negative Refraction Makes a Perfect Lens," Phys. Rev. Lett. **85,** 3966-3969 (2000).
5. D. O. S. Melville, and R. J. Blaikie, "Super-resolution imaging through a planar silver layer," Opt. Express **13,** 2127-2134 (2005).
6. H. Heinzelmann, and D. W. Pohl, "Scanning near-field optical microscopy," Appl. Phys. A **59**, 89 (1994).
7. B. Hecht, B. Sick, U. P. Wild, V. Deckert, R. Zenobi, O. J. F. Martin, and D. W. Pohl, "Scanning near-field optical microscopy with aperture probes: Fundamentals and applications," J. Chem. Phys. 112, 7761 (2000).
8. Z. Liu, J. M.Steele, W. Srituravanich, Y. Pikus, C. Sun, and X. Zhang, "Focusing surface plasmons with a plasmonic lens," Nano Lett.. **5**: 1726-1729 (2005).
9. L. Yin, V. K. Vlasko-Vlasov, J. Pearson, J. M. Hiller, J. Hua, U. Welp, D. E. Brown, and C. W. Kimball, "Subwavelength focusing and guiding of surface plasmons," Nano Lett. **5,** 1399-1402 (2005).
10. R. Rokitski, K. A. Tetz, and Y. Fainman, "Propagation of femtosecond surface plasmon polariton pulses on the surface of a nanostructured metallic film: space-time complex amplitude characterization," Phys. Rev. Lett. **95,** 177401 (2005).
11. A. Hohenau, J. R. Krenn, A. L. Stepanov, A. Drezet, H. Ditlbacher, B. Steinberger, A. Leitner, and F. R. Aussenegg, " Dielectric optical elements for surface plasmons," Opt. Lett. **30,** 893-895 (2005).
12. L. Feng, K. A. Tetz, B. Slutsky, V. Lomakin, and Y. Fainman, "Fourier plasmonics: diffractive focusing of in-plane surface plasmon polariton waves," Appl. Phys. Lett. **91,** 081101 (2007).
13. H. F. Ghaemi, T. Thio, D. E. Grupp, T. W. Ebbesen, and H. J. Lezec, "Surface plasmons enhance optical transmission through subwavelength holes," Phys. Rev. B **58**, 6779-6782 (1998).
14. J. D. Love, W. M. Henry, W. J. Stewart, R. J. Black, S. Lacroix, and F. Gonthier, "Tapered Single-mode Fibres and Devices Part 1: Adiabaticity Criteria," IEE Proc. J. **138**, 343-354 (1991).
15. R. J. Black, S. Lacroix, F. Gonthier, and J. D. Love, "Tapered single-mode fibres and devices - Part 2: Experimental and theoretical quantification," IEE Proc. J **138**, 355-364 (1991).
16. P. B. Johnson and R. W.Christy, "Optical constants of the noble metals," Phys. Rev. B **6,** 4370-4379 (1972).
17. Y. Jung, G. Brambilla, and D. J. Richardson, "Broadband single-mode operation of standard optical fibers by using a sub-wavelength optical wire filter," Opt. Express **16**, 14661-14667 (2008), http://www.opticsinfobase.org/abstract.cfm?URI=oe-16-19-14661.

1. Introduction

Light confinement is limited by diffraction and the ultimate spot size Δx is related to of the vacuum wavelength λ_0 and to the refractive index n of the medium where light propagates[1]:

#108998 - $15.00 USD Received 19 Mar 2009; revised 20 Apr 2009; accepted 21 Apr 2009; published 23 Apr 2009

$$\Delta x \geq \frac{\lambda_0}{2n} \tag{1}$$

In classical optics, sub-wavelength confinement has been achieved by using two high-refractive index slabs separated by a sub-wavelength gap in air [2]. The boundary conditions of the electrical field at the interface between the high refractive index medium and air allow for a strong field enhancement in the gap region. Still, since the field in the gap is the evanescent tail of the mode in the high refractive index medium, a considerable fraction of the power is located outside the gap.

Veselago's metamaterials [3, 4] can virtually focus light without any diffraction because of their negative refractive index. Practical implementations envisage the realization of "lens stacks" and are typically used for imaging [5]. They can achieve extraordinary resolution but no light localization within a small spot size has been demonstrated, yet. The well-known scanning near-field optical microscope (SNOM) tips are an alternative way to provide sub-wavelength light sources [6], but their transmissivity is very low, often in the order of 10^{-6} for a sub-100nm tip [7].

Surface plasmon polaritons (SPP) have been shown to be good candidates for sub-wavelength confinement because of their evanescent field nature. Various schemes have been proposed [8-12] but previous attempts in planar nanostructured materials have demonstrated a poor efficiency because of the difficulty to couple light into the nanostructures [13] used to generate SPP. Optical fiber tapers confine adiabatically light to the diffraction limit and provide an extremely regular field distribution within a relatively small area. Here the taper tip is nanostructured to efficiently excite SPP and confine light to sub-wavelength dimensions.

2. Device Manufacture

Figure 1 shows a schematic of the device manufacture. An optical fiber was firstly pulled to obtain an adiabatic taper (Fig. 1(a)) with a tip diameter of d~1.5 μm.

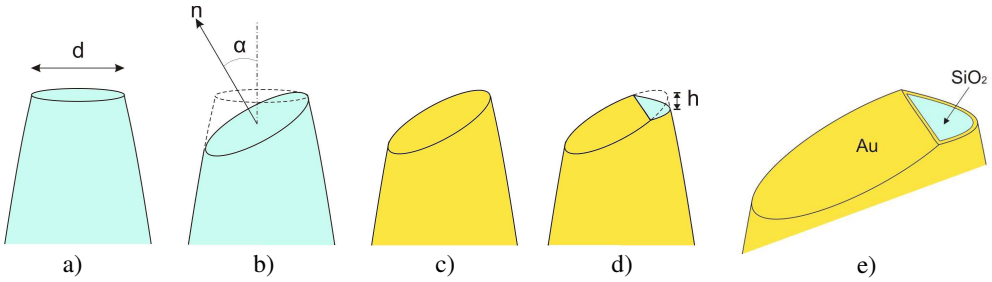

Fig. 1. Schematic of the device fabrication. a) A tapered fibre is manufactured from a singlemoded optical fibre; d is the taper tip diameter. b) First focused ion beam (FIB) milling.α is defined as the angle between the taper axis and the normal n to the cut. α represents the angle at which the light propagation constant along the newly formed surface matches the surface plasmon polariton (SPP) propagation constant. c) Chrome and gold coating. d) A second FIB milling generates the sub-wavelength window: h represents the distance between the cut and the coated fibre tip. E) Detail of the final device.

The optical fiber (NUFERN 780-HP) was singlemoded in the wavelength range 700-900 nm and had core diameter, cladding diameter and numerical aperture of 4.296 μm, 125 μm and 0.13, respectively. The fabrication of the optical fiber taper was carried out with a commercial pipette puller. CO_2 laser power and pulling velocity were optimized to achieve an optimum taper profile. Its slope in fact has to be slow enough to minimize the power loss and to adiabatically convert the fundamental mode in the fiber into a smaller mode guided by the cladding/air interface in the taper [14, 15]. Transmissivities larger than 98% are commonly registered in optimized adiabatic tapers.

#108998 - $15.00 USD Received 19 Mar 2009; revised 20 Apr 2009; accepted 21 Apr 2009; published 23 Apr 2009

The fiber taper tip was then cut (Fig. 1(b)) at an angle α suitable to excite SPP at the interface between gold and air. Fiber cleaving has been carried out at OpTek Systems Ltd. (U.K.) using a CO_2 laser based system having accuracy better than 0.1 degrees. SPPs are collective electronic excitations at metal surfaces by evanescent optical fields and occur only when light hits the surface at a very specific angle. The angle α was chosen to excite SPPs at the gold-air interface, thus the projection of the light wave vector on the surface k_α has to match the SPP propagation constant β. This condition yields:

$$\alpha = \arcsin\left(\frac{1}{n_{eff}}\sqrt{\frac{\varepsilon_{met}\varepsilon_{air}}{\varepsilon_{met}+\varepsilon_{air}}}\right) \tag{2}$$

where n_{eff} is the HE_{11} effective index, and ε_{met} and ε_{air} are the dielectric constants of gold [16] and air respectively. For the wavelength range 700-950 nm, Eq. 2 shows that the angle variation is around one degree within the whole wavelength range. To have better accuracies than 0.1 degrees, the tip was micro-structured with a focused ion beam (FIB) system. The sample was then covered with a few nanometers of Cr and with ~50 nm of Au (Fig. 1(c)). Cr was used as buffer layer between Au and silica to increase Au adhesion and long term stability. Finally a cut of 200 nm from the tip (represented by segment h in Fig. 1(d)) was made perpendicularly to the fiber axis using the FIB machine. A detailed vision of the nanostructured tip is shown in Fig. 1(e). This device had a sub-wavelength window (~150nm wide) used to demonstrate the improved light confinement at least in one dimension. The thin gold layer was used to generate SPP and confine them into a sub-wavelength region.

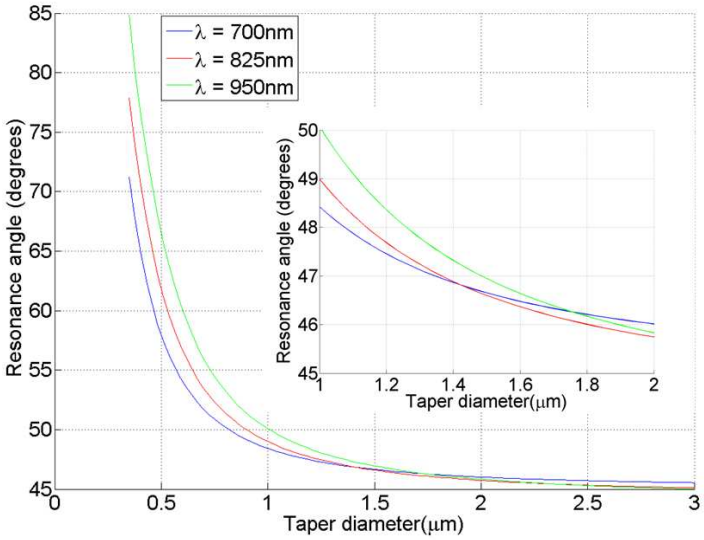

Fig. 2. Dependence of the resonance angle on the taper diameter for fiber tapers coated with gold. The inset shows a detail for taper diameters between 1 and 2μm.

SPP resonance conditions change with wavelength and tip diameter: Fig. 2 shows that the resonance angle α increases for decreasing tip diameters and increasing wavelengths. Since the effective index is decreasing with the taper tip diameter, Eq. 2 shows that the variation of α with the diameter is larger for smaller taper tips. For very small taper diameters, the mode effective index becomes very close to the air refractive index and the resonance angle approaches 90 degrees. In order to have bigger tolerance levels during the device fabrication, taper tips with 1μm diameter seem desirable. The inset shows the details for diameters in the 1-2μm range.

#108998 - $15.00 USD Received 19 Mar 2009; revised 20 Apr 2009; accepted 21 Apr 2009; published 23 Apr 2009

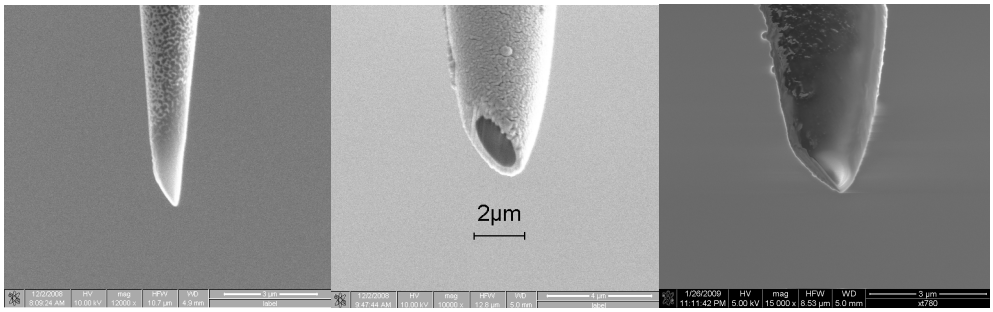

Fig. 3. Samples realized by focused ion beam (FIB) milling. The bright and the dark areas represent gold coated and bare silica regions, respectively.

Figure 3 shows some of the samples milled with the FIB system. In Fig. 3(b) the dark and bright regions correspond to the uncovered silica and the gold coating, respectively. Although Au has been deposited on the sample to generate and confine SPPs, it has a beneficial effect on the FIB milling: the conductive gold layer avoids the charge accumulation on the sample which can deflect the ion beam and considerably deteriorate the overall resolution. Figure 3c shows the final sample, cut at an angle α=46.3º.

3. Sample characterization

The sample transmission properties were characterized with the setup shown in Fig. 4.

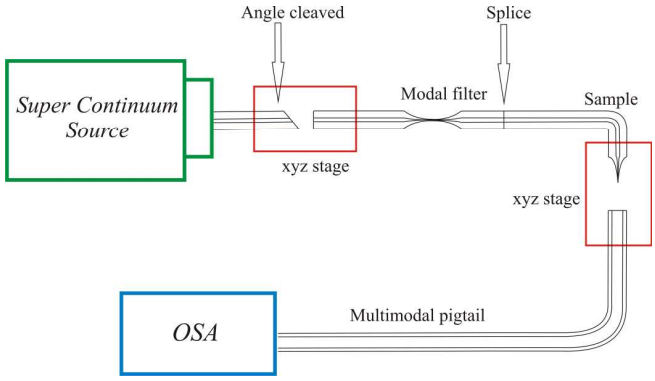

Fig. 4. Schematic of the set-up used to measure the prototype transmission efficiency: a supercontinuum source is coupled through a xyz stage to a modal filter, necessary to have single moded propagation along all the range of wavelengths considered. The filter is spliced to the sample and the transmitted light is collected by an OSA using a multimodal fiber.

400 fs, 50 nJ pulses in the wavelength range 650-1800 nm were injected in the sample by a supercontinuum source (Fianium). Coupling optimization was achieved using a xyz stage. A micro-wire modal filter [17] was inserted before the sample: although the fiber second mode cut-off was at 730 nm, the filter ensured that no power was propagating in the second mode at any wavelength. In fact high order modes have different effective indices, thus SPP excitation occurs at different resonance conditions (Eq. 2). Light propagating through the sample was then collected using a multimodal fiber connected to an OSA.

#108998 - $15.00 USD Received 19 Mar 2009; revised 20 Apr 2009; accepted 21 Apr 2009; published 23 Apr 2009

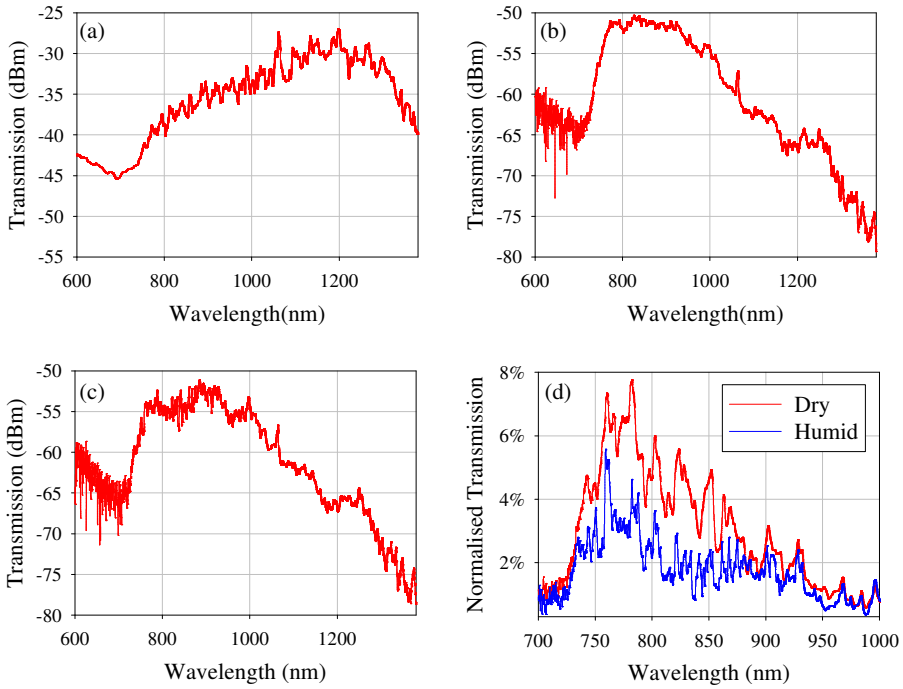

Fig. 5. Spectra of the supercontinuum source with the microwire mode filter (a), and with the sample in dry (b) and humid (c) environments. Spectra (b) and (c) have been normalised with respect to (a) and are reported in red and blue in (d).

Measurement results are presented in Fig. 5. Figure 5(a) shows the modal filter spectral response, used to normalize the sample spectrum and to remove any wavelength dependence related to the source, to the detector and to the modal filter itself. Figure 5(b) shows the sample spectrum in dry air: a big resonance peak is clearly visible at ~780nm. When the sample is placed in a humid environment, SPP resonance conditions change and the peak is attenuated (Fig. 5(c)). Figure 5(d) shows the normalized peaks in dry (red line) and humid (blue line) environments, evaluated from the ratio between the spectra in Figs. 5(b) and 5(a) and between the spectra in Figs. 5(c) and 5(a) respectively. The noise at short wavelengths was ascribed to the low source power and OSA sensitivity at these wavelengths. High frequency peaks have been associated to the supercontinuum source. The broad peak at 900nm has also been associated to the supercontinuum source; indeed, since it is unaffected by changes in the local environment this broad peak cannot be related to SPP. The maximum transmissivity recorded in Fig. 5(d) was ~-11dB≈8% at λ=780 nm, nearly one order of magnitude higher than that observed at the peak tails (at 700nm and 950nm). Since there is no SPP contribution, the output measured at the tails represents the power transmitted because of pure geometrical reasons.

Simulations have been carried out to evaluate this power fraction assuming a circular waveguide partially covered with gold (shown in Fig. 6(a)). The extent of the gold region is uniquely defined by the parameter ρ. Although the geometry of the real sample is far more complicated than the schematic shown in Fig. 6 (the taper has a conical profile and the cut is diagonal to the taper axis, Fig. 1(d)), Fig. 6 could be considered as the projection of the diagonal surface on a plane perpendicular to the taper axis. The parameter ρ is evaluated from the real structure. Measuring the sample dimensions of Fig. 3(c) and using simple geometrical considerations, the sample was approximated to a circular waveguide with radius a=0.79 μm and ρ=0.636 μm. The output power at λ=780nm (maximum of Fig. 5(d)) was evaluated integrating the Poynting vector over the uncovered surface of the waveguide of Fig. 6(a).

#108998 - $15.00 USD Received 19 Mar 2009; revised 20 Apr 2009; accepted 21 Apr 2009; published 23 Apr 2009

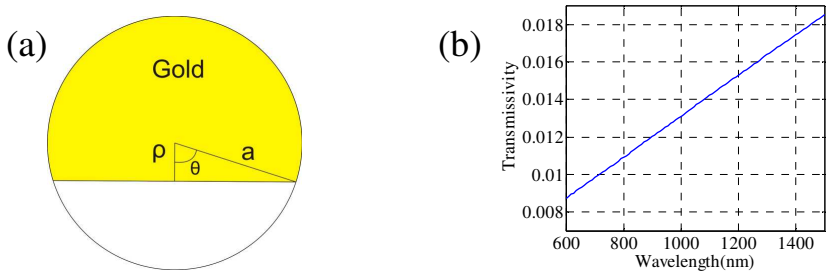

Fig. 6. (a) Geometrical structure of an equivalent waveguide used for simulations. Light is emitted only through the white (uncovered) section. (b) Simulated transmission from the uncovered taper window because of simple geometrical considerations.

The simulation results are shown in Fig. 6(b), where the power is normalized to the total power injected in the fiber. At a wavelength of 780 nm, the transmissivity is -19.71dB (~1.07%), about one order of magnitude smaller than the measured value of -11dB (~8%) and considerably larger than the values reported for SNOM tips of comparable size [7]. This enhancement has been ascribed to the SPP enhancement. Moreover for λ=984 nm (which is out of the resonance peak) the Matlab simulation provided a transmissivity of ≈1.3%, comparable with the measurement of ≈1.07% of Fig. 5d. Although a transmission increase of 0.3% has been predicted in the wavelength range 700-1000nm (Fog. 6(b)), this effect is not readily visible in the experimental results (Fig. 5(d)), possibly because of the poor long term stability of the supercontinuum source and/or the relatively low signal/noise ratio.

The great majority of transmission effectively occurs only at the sub-wavelength aperture (Fig. 1(c)). No transmission has been observed in an Au-coated tip without aperture. Moreover, from the value of the gold refractive index at 780 nm [16], the critical angle for transmission at the interface between silica and gold results to be 5.80º. If the very thin layer of gold is neglected, the critical angle at the interface between silica and air is 43.46º. In both cases α of the sample of Fig. 5(d) is bigger than the critical angle, meaning that the light can not be transmitted through the coated area.

4. Conclusions

In conclusion, efficient sub-wavelength confinement has been proved at 780nm by using surface Plasmon polaritons at the tip of an adiabatic optical fiber taper. An order of magnitude improvement in the device transmission has been demonstrated at the surface plasmon resonance wavelength. Effective confinements to 10nm or smaller can be envisaged by decreasing the aperture size.

Acknowledgments

The authors thank the Engineering and Physical Sciences Research Council UK (EPSRC) for financial support; GB gratefully acknowledges the Royal Society (London, UK) for his Research Fellowship.

#108998 - $15.00 USD Received 19 Mar 2009; revised 20 Apr 2009; accepted 21 Apr 2009; published 23 Apr 2009